Okhotsk Sea and Polar Oceans Research 6 (2022) 27-35

https://doi.org/10.57287/ospor.6.27

Article

Sea ice variability along the Okhotsk coast of Hokkaido based on long-term JMA meteorological observatory data

Takahiro TOYODA[1], Yoshiteru KITAMURA[1], Ryohei OKADA[2], Kanichiro MATSUMURA[3], Kensuke K. KOMATSU[1], Kei SAKAMOTO[1], L. Shogo URAKAWA[1] and Hideyuki NAKANO[1]

[1]*Department of Atmosphere, Ocean, and Earth System Modeling Research, Meteorological Research Institute, Japan Meteorological Agency, Tsukuba, Japan*
[2]*Atmosphere and Ocean Department, Japan Meteorological Agency, Tokyo, Japan*
[3]*Faculty of Bioindustry, Tokyo University of Agriculture, Abashiri, Japan*

(Received September 29, 2021; Revised manuscript accepted December 21, 2021)

Abstract

Long-term sea ice observation data at the Japan Meteorological Agency observatories along the Okhotsk coast of Hokkaido were analyzed. The observations at the Abashiri Local Meteorological Observatory largely explained the variations at other sites along much of the Okhotsk coast on a time scale longer than a few days. Interannually, variations of the maximum sea ice areas in the whole and southern Sea of Okhotsk were largely reflected in the yearly accumulated sea ice concentration (SIC) and sea ice duration variations at the observatories. A comparison with several indices for the North Pacific climate variability suggested that the North Pacific Index (NPI) is a robust indicator of the recent (after the 1980s) sea ice variations in the Sea of Okhotsk on a decadal time scale. Specifically, variations in the first sea ice appearance date at the observatories resulted from variations in the Aleutian Low with meridional wind anomalies over the Sea of Okhotsk and the air temperature around Japan in January; variations in the final disappearance date resulted from the Aleutian Low variations, and the resulting sea ice cover variations in the Sea of Okhotsk except for the Siberian coast affected the air temperatures in April. These factors influenced the sea ice duration. A strong linkage was found between variations in the local sea ice (along the Hokkaido coast) and large-scale fields, which will help improve our understanding of the sea ice extent and retreat variability over the Sea of Okhotsk and its linkage to the North Pacific climate variability.

Key words: sea ice, Sea of Okhotsk, Hokkaido, climate variability, JMA meteorological observatory

1. Introduction

The marginal Sea of Okhotsk in the western North Pacific is characterized by its seasonal sea ice cover. Sea ice is mainly formed in the northern and northwestern shelf regions due to the winter northwesterly monsoon bringing cold air from Siberia. It then extends southward, particularly in the western part along the eastern coast of Sakhalin, and eventually reaches the northeastern coast of Hokkaido facing the Sea of Okhotsk in late January (Fig. 1a). The existence of sea ice is highly influential for local communities around the Sea of Okhotsk (*e.g.*, Shirasawa *et al.*, 2005). It is also important for larger-scale atmospheric variability around the North Pacific (*e.g.*, Honda *et al.*, 1996, 1999; Kawasaki *et al.*, 2021) and ventilation of the North Pacific Ocean (*e.g.*, Nakamura *et al.*, 2006).

Large interannual variability in the sea ice extent in the Sea of Okhotsk has been detected, as well as a decreasing trend (> 10% per decade; *e.g.*, Parkinson and Cavalieri, 2008), which would include the feedback from atmosphere and ocean variations (*e.g.*, Ohshima *et al.*, 2014). The variation in the sea ice extent over the Sea of Okhotsk influences local sea ice evolution such as its appearance along the Hokkaido coast. Aota (1999) presented a long-term decreasing tendency of the sea ice amount (see Section 3) as observed at the Abashiri Local Meteorological Observatory from 1892, linking it to atmospheric warming. Tachibana *et al.* (1996) found that an abrupt reduction of the sea ice cover in the southern part of the Sea of Okhotsk occurred at the end of the 1980s, resulting from a weakening of the wintertime Aleutian Low; the reduced sea ice condition has continued (at least until 1994 in their study). Takahashi *et al.* (2011) presented good correlations between the sea ice duration and local air temperature at four sites along the coast of Hokkaido.

Yamazaki (2000) discussed how the winter sea ice area in the Sea of Okhotsk is mostly explained by the wind (as represented by the sea level pressure (SLP) difference between 150°E, 45°N and 170°E, 60°N), the air temperature (at 140°E, 55°N and the 850 hPa height), and the sea ice area at the beginning of January. Regarding the January sea ice area, Ohshima *et al.* (2006) highlighted the importance of the air

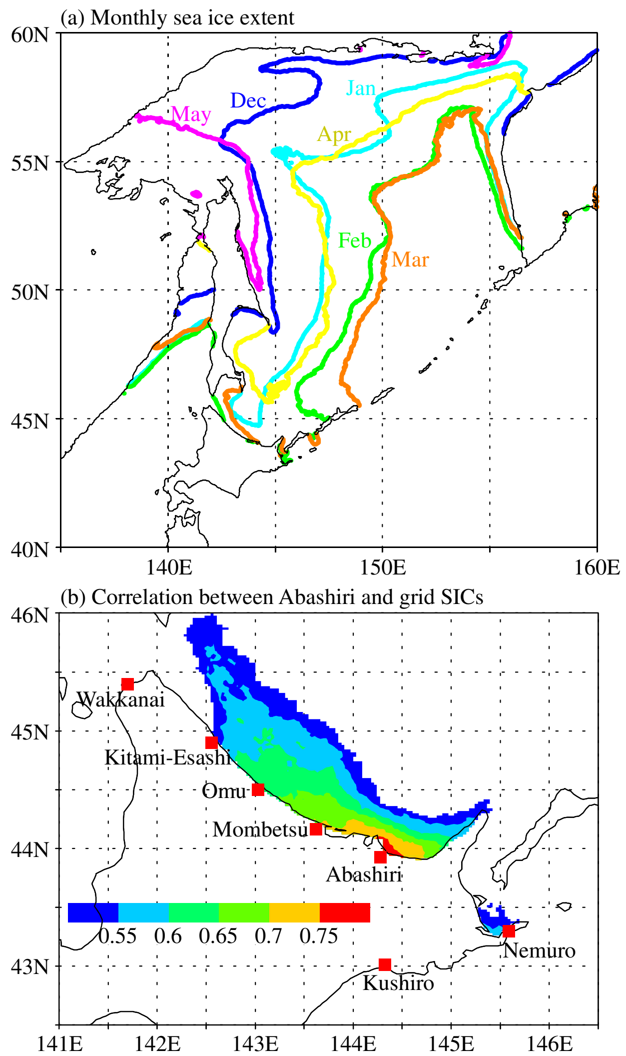

Fig. 1 (a) Monthly sea ice extent (contours of grid SIC = 0.3) averaged over 1977–2019. (b) Locations of JMA observatories and distribution of daily-basis correlation coefficients between the Abashiri and grid SICs. (N = 700–800 approximately).

temperatures (and hence heat fluxes) in the ice formation region in the fall (October–November) and also suggested that the oceanic conditions affect the advances in the sea ice extent in the downstream region, and hence the maximum extent. Thus, several processes affect the time evolution of the sea ice distribution, particularly the start and end dates of the sea ice existence in the season and the accumulated concentration and duration of the sea ice at coastal sites in the downstream region (*e.g.*, Hokkaido), which requires further investigation.

In the present study, we focused on the local sea ice variability along the Okhotsk coast of Hokkaido. In doing so, we used the long-term archives of the daily sea ice concentration (SIC) observations at the meteorological observatories of the Japan Meteorological Agency (JMA). This set is one of the longest observational records that can be used for climate study, at least near the Okhotsk coast of Hokkaido. We individually analyzed the start and end dates and accumulated sea ice cover (Aota *et al.*, 1988) and their relationship to the large-scale atmospheric fields and North Pacific climate indices. Particular attention was paid to how the observations at the Abashiri Local Meteorological Observatory represent the regional sea ice cover, considering that several other observatories terminated observation of the sea ice component. Since the meteorological features are similar among the northern and southern areas and southernmost Hokkaido coast of the Sea of Okhotsk in terms of high sensitivity to atmospheric variability such as extratropical cyclones and polar jets, a global outlook of the Sea of Okhotsk is provided in association with the sea ice variability. The results would be useful for understanding the sea ice variability in the southern downstream region.

2. Data

We used the daily drift and total (the latter includes locally formed ice) SIC data based on direct observations at the JMA observatories along the coast of Hokkaido: Wakkanai, Kitami-Esashi, Omu, Mombetsu, Abashiri, Nemuro, and Kushiro (Fig. 1b). The data periods differ among the sites and variables (starting from the 1950s; see Fig. 2). These data are available online at https://www.data.jma.go.jp/gmd/kaiyou/db/seaice/hokkaido/hokkaido_ice_sequence.html. Quality controls (such as for data with an inconsistency of drift ice > total ice) were conducted based on the continuity of time series and consistency with local air temperatures (subjectively). For the start and end dates of the local sea ice existence, longer records than for the SIC are available (*e.g.*, from 1946 at Abashiri).

Daily (5 days) gridded SIC data based on satellite measurements in the Sea of Okhotsk are routinely produced for operational use by the JMA. The horizontal resolution is 1/33° zonally and 1/50° meridionally (about 2 km). We used the data from December 1977 to December 2019. See https://www.data.jma.go.jp/gmd/kaiyou/db/seaice/okhotsk/okhotsk_extent.html. We refer to these data as “grid SIC” data in this study.

Sea ice indices for the Sea of Okhotsk are defined in this study as yearly integrations of the above-described local SIC data and yearly maximum area coverages based on the grid SIC data (see Section 3).

We also used the daily (5 days) mean surface air temperature and wind direction and speed data at the same observatories. In addition, we used a winter (December–February) time series of the North Pacific Index (NPI; Trenberth and Hurrell, 1994) and West Pacific pattern (WP; Wallace and Gutzler, 1981), Pacific Decadal Oscillation (PDO; Mantua and Hare, 2002), North Pacific Gyre Oscillation (NPGO; Di Lorenzo *et al.*, 2008), and Monsoon (MOI; Watanabe, 1990) indices, as measures of the intensities of large-scale climate modes in the North Pacific. These data are available online at https://www.jma.go.jp/jma/menu/menureport.html except for the WP index, which can be obtained online at https://www.cpc.ncep.noaa.gov/data/teledoc/wp.shtml.

The JRA-55 atmospheric reanalysis (Kobayashi *et al.*, 2015) dataset is available at http://jra.kishou.go.jp/JRA-55/index_en.html.

The merged satellite and in situ sea surface temperature (SST) dataset of the JMA (MGDSST; Kurihara *et al.*, 2006) is available at http://ds.data.jma.go.jp/gmd/goos/data/rrtdb/jma-pro/mgd_sst_glb_D.html.

3. Results

The meteorological observatory data are derived from direct (visual) observations at 9:00 a.m. local time within the range of 20 km from the observatories (relatively weighted on the 5 km range; personal communication with Fumitake Shido). The satellite-based grid SIC data provide information on the spatiotemporal variability (with a 2 km resolution) but inevitably suffer from noise such as that due to cloud cover and coastal effects (*e.g.*, Yamazaki, 2000). As shown in Fig. 1b, the correlation between the Abashiri and grid SICs was lower than 0.8 (grid SICs on every five days and Abashiri SIC on the same days were compared; data were not used when both SICs = 0). Thus, these datasets are not exactly consistent at the observatory site (on the nearest grid to Abashiri for the grid SICs). Nevertheless, a relatively large correlation (at a similar level to the co-located value) can be seen along a large part of the Okhotsk coast of Hokkaido and upstream of the sea ice advection near Sakhalin. In addition, relatively high correlations along the Hokkaido coast against the grid SICs were obtained for other observatory data at Kitami-Esashi, Omu, Mombetsu, and also Nemuro (not shown). These results suggest that the SIC variations on a time scale of five days along the Okhotsk coast (between Kitami-Esashi and Shiretoko Peninsula approximately) were largely captured by the Abashiri observations, which is consistent with previous studies (*e.g.*, Aota *et al.*, 1988; Nakamura, 1996). Actually, high correlation coefficients with the Abashiri data were obtained for the Kitami-Esashi (0.61), Omu (0.69), Mombetsu (0.74), and Nemuro (0.65) data, respectively (daily values were used; N = 5000–6000). In contrast, the observations at Wakkanai and Kushiro showed much more confined correlated areas with the grid SIC data and smaller correlations with the Abashiri data (0.32 and 0.06, respectively).

Figure 2 depicts the yearly time series. Although there existed differences in detail, the maximum sea ice areas in the whole and southern (<50°N) Sea of Okhotsk generally covaried (Fig. 2a; R = 0.81). Note that variations in the northern area as well as the southern area contribute to the whole area variations, whereas Aota *et al.* (1988) suggested much smaller interannual variations in the northern part than in the southern part for the period of 1971–1985. In addition, a gross similarity to these time series (*e.g.*, relatively low in the first half of the 1990s; further discussed later with Fig. 3) can be seen for the time series of accumulated SICs, i.e., time integral of daily SICs with a unit [SIC (%) day] (Aota *et al.*, 1988) at the observatories, Kitami-Esashi, Omu, Mombetsu, Abashiri, and Nemuro. Since the variations in the accumulated SICs for the drift and total ice (thin and thick lines, respectively) were generally compatible (except for Nemuro), we hereafter use the total ice SICs at Abashiri as generally representing the variations in the other observatory data (Kitami-Esashi, Omu, Mombetsu, and Nemuro). The variations were rather different at Wakkanai and Kushiro.

It should be noted that although we defined the southern part as south of 50°N following previous studies (*e.g.*, Aota *et al.*, 1988; Aota and Ishikawa,

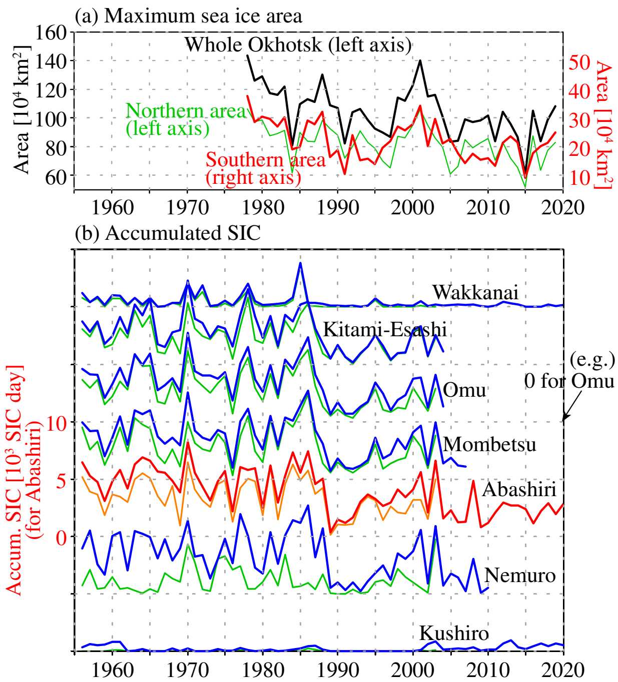

Fig. 2 (a) Yearly maximum sea ice areas in the Sea of Okhotsk from the grid SIC data for the whole (black; left axis), northern (>50°N; green; left axis), and southern (<50°N; red; right axis) areas. (b) Yearly time series of accumulated SICs at the meteorological observatories. Lines are vertically shifted by 5×10^3 [SIC day] (interval of the horizontal dotted lines) between sites. Red (orange) line indicates accumulated total (drift) SIC for Abashiri. Blue (green) lines are for the other sites, individually.

1993; Tachibana *et al.*, 1996) and analyzed the yearly maxima of the daily (5 days) sea ice area in this study (Fig. 2a), the correlation between the whole and southern Okhotsk sea ice areas becomes much smaller when we use the sea ice area of a fixed day or period (1 December–14 March by Tachibana *et al.* (2016); 15 February by Toyota *et al.* (2021)) and the southern part definition as south of 46°N (Toyota *et al.*, 2021). In addition, a negative correlation between the whole sea ice area in the Sea of Okhotsk and the sea ice amount along the Hokkaido coast was suggested for the data before the 1980s in previous studies (see Honda, 2007). Whether or not this relationship has recently changed is outside the scope of this study. At least, it might depend on the definition of the sea ice area as described above.

To investigate the above sea ice quantities of the Sea of Okhotsk in relation to the large-scale climate mode variations in the North Pacific, particularly their decadal phase changes (*e.g.*, Tachibana *et al.*, 1996), we compared these quantities (sea ice indices) with the North Pacific climate indices (for December–February; Fig. 3a). Note that these climate mode indices are not independent of each other: for example, both the NPI and PDO (based on SLP and SST patterns, respectively) are associated with variations in the Aleutian Low strength, whereas the WP and NPGO are both associated with variations in the meridional position of the Aleutian Low (*e.g.*, Toyoda *et al.*, 2017). As discussed by Tachibana *et al.* (1996), the sea ice indices (Fig. 3b) decreased abruptly around 1989/1990, which corresponded to large changes in the climate mode indices, *e.g.*, a phase shift of the PDO. After that, the sea ice area in the Sea of Okhotsk increased and reached a peak in 2001 (Fig. 2a; 3b), which corresponded to negative phases of the NPGO and NPI. Note that the above simultaneous comparisons do not indicate causal relationships.

As suggested by Yamazaki (2000), several climate index patterns associated with the Aleutian Low variability can affect the sea ice amount in the Sea of Okhotsk. We calculated the running correlations with a 21-year window between the sea ice indices of the Sea of Okhotsk and indices of the North Pacific climate mode variabilities (*e.g.*, the value in 2000 denotes a correlation during the period of 1990–2010). For the whole and southern sea ice maxima, the correlations with the NPGO and NPI were relatively large; the correlations with the PDO were low, particularly for the index of the whole Sea of Okhotsk (lower than 90% and 95% confidence levels of 0.37 and 0.43, respectively).

Longer records can be compared by using the accumulated SICs at Abashiri. In the first half of the 1970s, the 21-year running correlations of the accumulated SIC with both the PDO and NPI were low. The correlation with the PDO increased afterward and

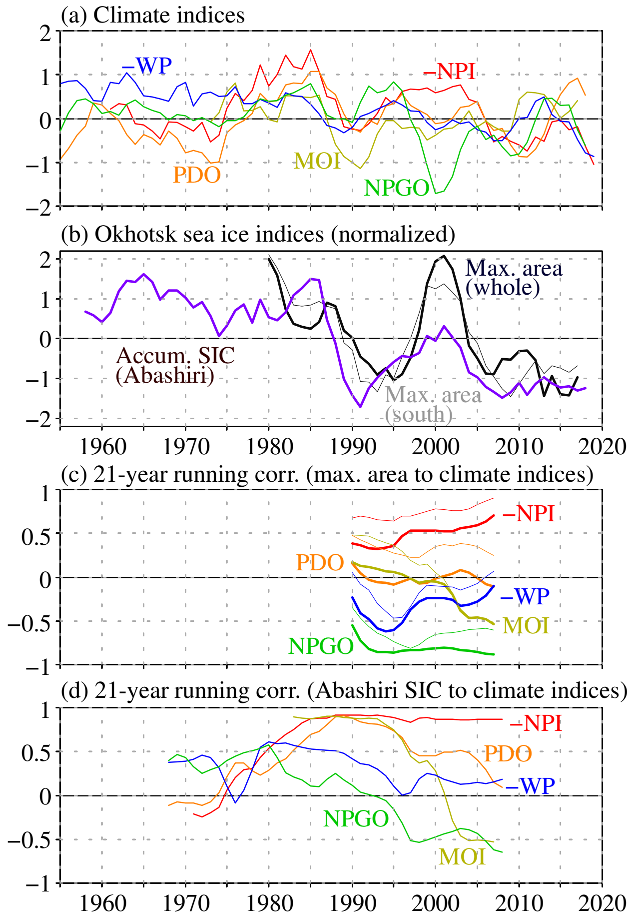

Fig. 3 (a) Yearly time series of the NPI (red; inverse in sign), WP (blue; inverse in sign), PDO (orange), NPGO (green), and MOI (dark yellow) indices for December–February. (b) Time series of normalized (by individual standard deviations) maximum sea ice area (black and gray lines for the whole and southern Sea of Okhotsk, respectively) and accumulated SIC at Abashiri (purple). 5-year running mean values are plotted for (a, b). (c) Running correlations with a 21-year (±10 years) window between the climate indices and maximum sea ice area for the whole and southern (thick and thin lines, respectively) Sea of Okhotsk. (d) Same as (c) but with correlations between the climate indices and accumulated SIC at Abashiri.

reached a peak around 1990, corresponding to the abrupt ice area reduction. The correlation with the NPI (inversed in sign) also increased during the 1980s and kept a high (significant) level after the late 1980s. This was in contrast to the correlation with the PDO, which gradually decreased after about 1990. The MOI also decreased after about 1990 and became negative in the early 2000s. This change in sign was also seen in the correlation of the maximum areas (Fig. 3c). The correlation with the NPGO was about +0.5 during the late 1960s and 1970s. It then decreased during the

1980s and 1990s, reached nearly zero around 1990, and stayed at about −0.5 after the late 1990s. From the correlations with the NPGO (Figs. 3c, d), the relationship between the maximum area and Abashiri SIC greatly changed in the 1980s to early 1990s, which can also be seen in the time series of these sea ice indices (Fig. 3b). The correlation with the WP was relatively high in the early 1970s and 1980s; it was low in the mid 1970s and after the 1990s. In summary, although the decadal-scale relationships of the sea ice indices to the North Pacific climate indices varied with time, the NPI was a robust indicator of the sea ice variations in the Sea of Okhotsk after the 1980s. In the 1970s and after the late 1990s, the correlation with the NPGO became relatively high but the signs were different between these periods. The period with a relatively high correlation with the PDO was limited to around 1990.

The duration of the sea ice existence can be another measure for the yearly sea ice influence, which might be more important to local communities (*e.g.*, fishery) than the accumulated SIC. As shown in Fig. 4a, the variations in the yearly sea ice duration at Abashiri mostly corresponded to those in the accumulated SIC and, again, the variations were similar along a large part of the Okhotsk coast (Kitami-Esashi, Omu, Mombetsu, Abashiri, and Nemuro). Thus, one measure at a site can largely substitute the others among these sites.

The sea ice duration is determined by the start and end dates with the sea ice within the visibility from the site. At Abashiri, the first appearance generally occurred in January (Fig. 4c) and the final disappearance largely occurred in April during the whole records but the number of years with the end date in March and April recently became equivalent (Fig. 4b). Around 1989/1990, both the delay in the start date and advance in the end date contributed to the short duration. After this period, on the other hand, this relationship with opposite signs was not seen: for example, the start date in 1993 was delayed to February, whereas the end date was also delayed to May. As described above, the average end date (red line for 5-year running mean) became noticeably earlier. Thus, these start and end date variations contributed differently to the recent total duration change. Since the total duration basically captures variations in the accumulated SIC and maximum sea ice area at least on a decadal scale as described above, the investigation of the start and end dates at the local site would provide useful information on the advance and retreat of the sea ice over the Sea of Okhotsk.

Based on the date ranges (Figs. 4b, c), we investigated the atmospheric fields in January for the start date and those in April for the end date. The monthly mean surface air temperatures at the same observatory (Abashiri) were well correlated with the start and end sea ice date variations (Fig. 5), i.e., the delayed start date and early end date, when the surface air temperature is relatively high in that month. Note that we also investigated the local wind fields (speed and direction), but variations related to the start and end dates were not found, as discussed by Aota *et al.* (1988) for the period of 1969–1988.

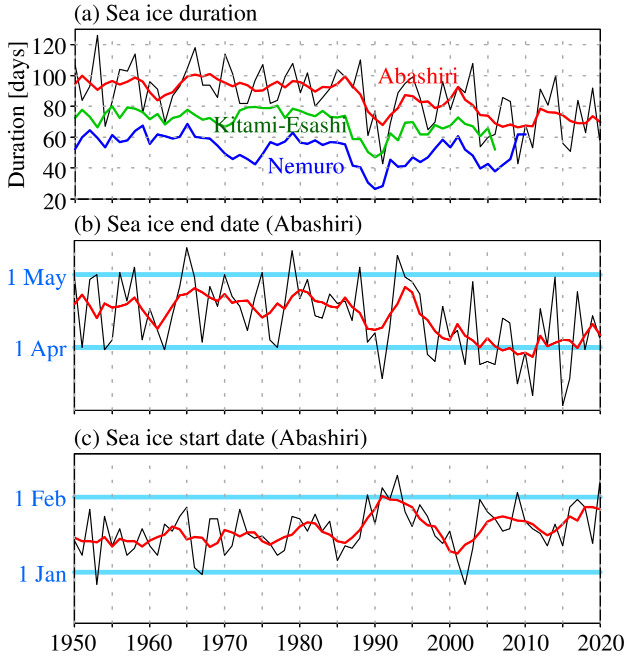

Fig. 4 (a) Time series of yearly durations (from December of the previous year) of the sea ice existence. Black and red lines denote the unsmoothed and 5-year running mean time series, respectively, at Abashiri. 5-year running mean plots are also shown for Kitami-Esashi (green) and Nemuro (blue). (b, c) Start (c) and end (b) dates of the sea ice existence at Abashiri. Unsmoothed and 5-year running mean values (black and red, respectively) are plotted. The y-axis denotes the date of the year (including December of the previous year in (c) which advances upward.

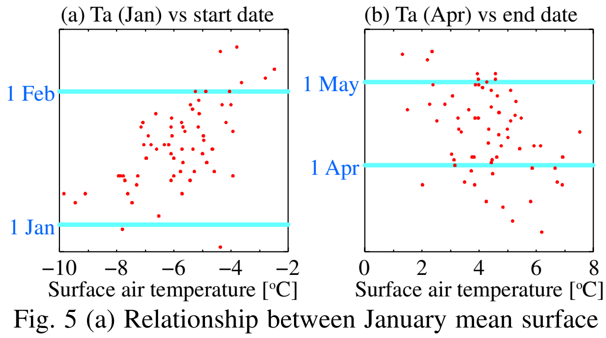

Fig. 5 (a) Relationship between January mean surface air temperature (Ta) and the sea ice start date at the Abashiri Local Meteorological Observatory. (b) Same as (a) but for the April mean surface air temperature and the sea ice end date.

To investigate the relationship between these dates and large-scale fields, we first examined the grid SICs in January and April regressed to the start and end dates, respectively (Fig. 6). Note that normalized date time series were used (mean and standard deviation values of the original start and end dates were 20.5 January ±9.0 days and 10.5 April ±15.8 days, respectively, during the overlapping period with the grid SIC data 1978–2019); hence, the SIC variations corresponding to one standard deviation of the date variations are presented. In January, negative values were distributed broadly over the Sea of Okhotsk (Fig. 6a). Thus, SICs over the whole sea ice region decreased with the delay of the sea ice start dates in the downstream region along the Okhotsk coast of Hokkaido. In April, positive SIC anomalies spread over most of the Sea of Okhotsk, whereas negative values were seen in the northwestern shelf region along the Siberian coast (Fig. 6b).

We next examined large-scale atmospheric fields (from JRA-55) in relation to the start and end dates. The regressions of the January SLPs to the start date (Fig. 7a) exhibited a weakening of the Aleutian Low (positive anomalies). This distribution is generally consistent with the result presented by Tachibana *et al.* (1996; for January–February). In association with these SLP anomalies, southerly wind anomalies were seen over the Sea of Okhotsk (Fig. 7a), which means a weakening of the northerly winds that are important to the sea ice advance (Kimura and Wakatsuchi, 1999; Shevchenko *et al.*, 2004). At the 850 hPa height, warm anomalies (>1°C) existed around Japan including the Okhotsk coast (Fig. 7b). At the surface, there were warm anomalies in the sea ice formation region along the Siberian coast, in addition to anomalies similar to those at the 850 hPa height (Fig. 7c). The surface turbulent heat flux regressions showed positive

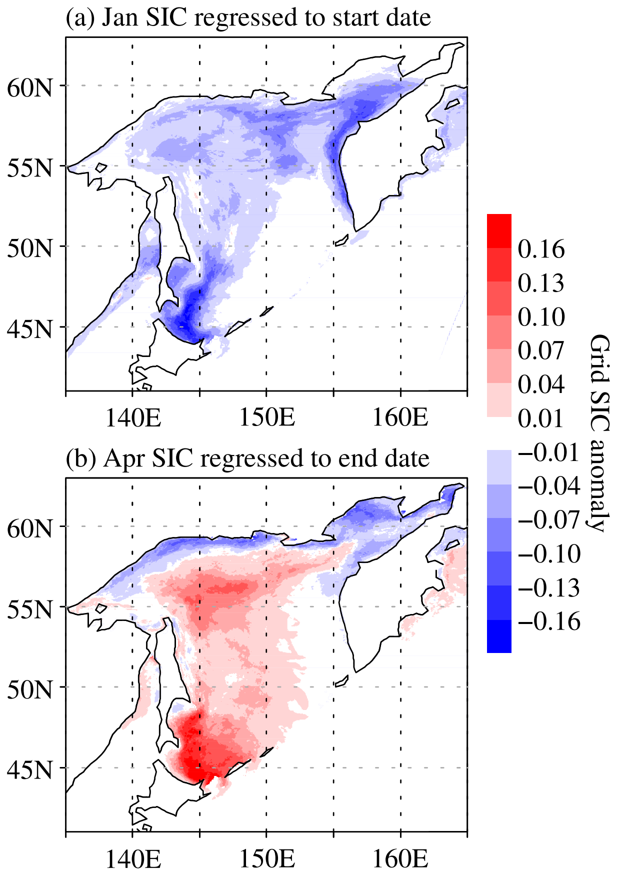

Fig. 6 (a) Regression distribution of the January grid SICs to the sea ice start date variations at Abashiri. (b) Same as (a) but with regression of the April grid SICs to the end date variations.

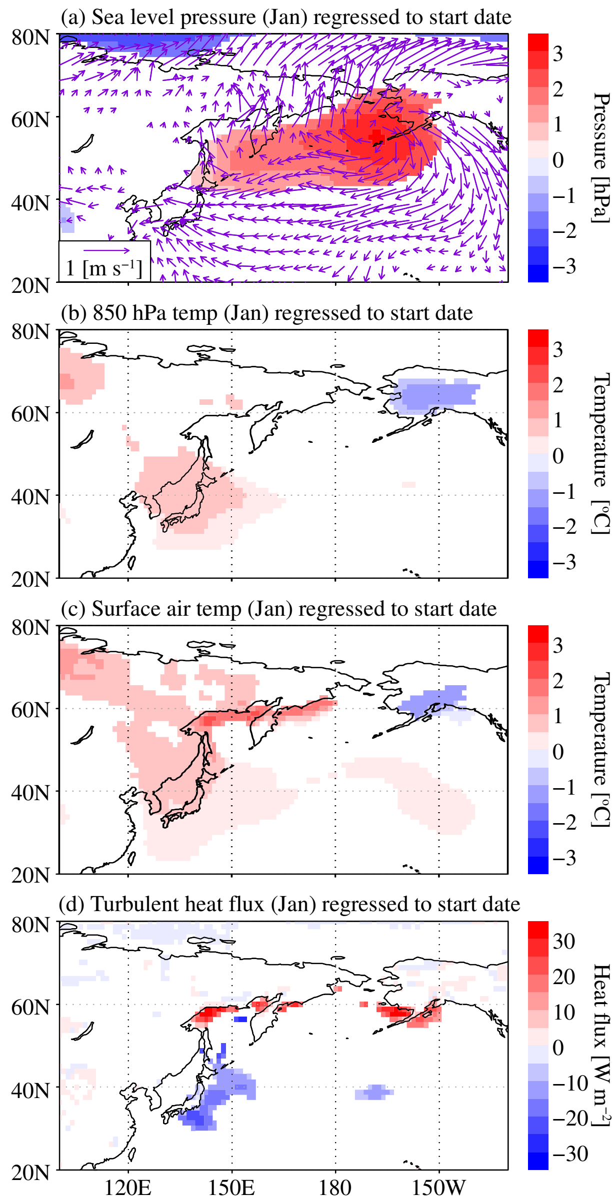

Fig. 7 Regression distribution of the January atmospheric fields (JRA-55) to the sea ice start date variations at Abashiri. (a) SLP (shading) and surface wind (arrows). (b) 850 hPa temperature. (c) Surface air temperature. (d) Surface turbulent (sensible plus latent) heat flux (positive upward). Only significant values at a 95% confidence level are shaded.

(upward) flux anomalies along the Siberian coast, which work to enhance the ice formation (partly recovering the shortage), and negative (downward) heat flux anomalies in the southern Sea of Okhotsk, which work to delay the start date by reducing the cooling at the ice–water surface. These results suggested that both the weakening of the northerly winds (due to the weakening of the Aleutian Low) and relatively warm temperatures around Japan (possibly affected by the weakening of the westerly jet) contributed to the delay of the start date and basin-scale smaller SICs in January (Fig. 6a).

As pointed out (but not analyzed) by Aota *et al.* (1988) and Yamazaki (2000), the oceanic conditions might affect the advance of the sea ice extent in the downstream region. Figure 8 shows the relationship between the start dates and SSTs in December, generally before the sea ice appearance. On the grid nearest to Abashiri, a weak but significant (95% confidence level) correlation of the start dates was obtained with the mean SSTs in December (red dots in Fig. 8a), whereas the correlation with the November SSTs (blue) was rather low. In addition, the relatively high correlation with the December SSTs was distributed along the Hokkaido coast through the Soya Strait (Fig. 8b). This might suggest the influence of the Soya warm current, which on average weakens greatly from November to January (Ohshima *et al.*, 2017) and requires further investigation in the future.

On average (climatology), the Aleutian Low weakens and shrinks to the north in April relative to January. Thus, the negative SLP regressions to the end date in April as shown in Fig. 9a indicate that when the end date is delayed, the relatively strong Aleutian Low is maintained, leading to the northerly wind anomalies over the Sea of Okhotsk.

The air temperature anomalies over the Sea of Okhotsk were rather small at the 850 hPa height (Fig. 9b), whereas cold anomalies were remarkable at the surface (Fig. 9c). Little influence of the sea ice existence on the 850 hPa temperature relative to the near-surface temperature is consistent with previous studies (see Honda, 2007). The heat flux anomalies were negative (Fig. 9d), reducing the upward heat release (*e.g.*, Ohshima *et al.*, 2003). Hence, the positive SIC anomalies (Fig. 6b) cooled the surface air (Fig. 9c). This is particularly seen in the northern Sea of Okhotsk with relatively large SIC anomalies (Fig. 6b). Note that the negative heat flux anomalies were more largely distributed to the south although they were not significant (not shown). Thus, the candidate cause of the delay of the end date was the northerly wind anomalies due to the relatively strong Aleutian Low for April, particularly in the western part. In addition, these wind anomalies generated relatively low SICs along the Siberian coast and relatively high SICs just to the south (Fig. 6b).

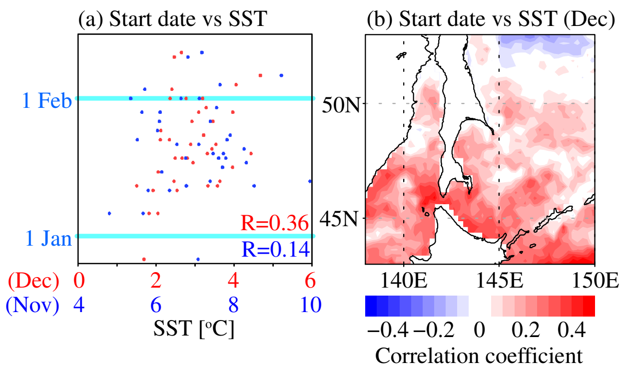

Fig. 8 (a) Scatter plots of the start days and monthly mean SSTs for November (blue) and December (red) on the Abashiri grid. (b) Distribution of correlation coefficients between the start day at Abashiri and the December mean SSTs.

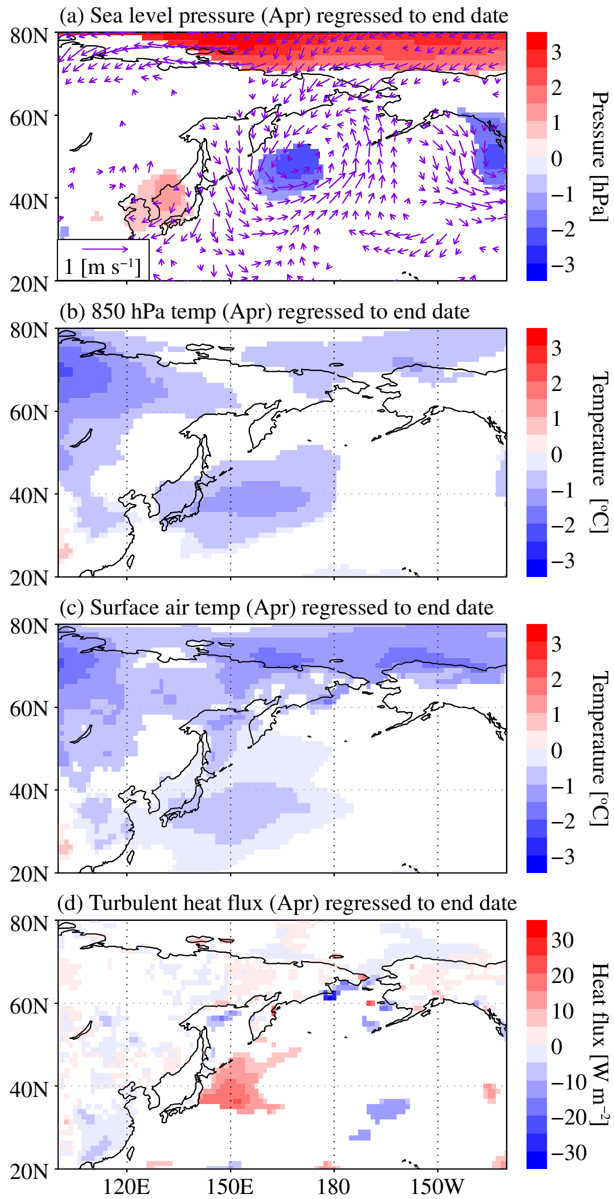

Fig. 9 Same as Fig. 7 but with regression of the April atmospheric fields to the end day variations.

4. Conclusion

We analyzed the sea ice observation data at the JMA meteorological observatories along the Okhotsk coast of Hokkaido. On a time scale longer than a few days, the observations at the Abashiri Local Meteorological Observatory largely explained the variations at other sites along the coast (Kitami-Esashi, Omu, Mombetsu, and Nemuro). This was also supported by correlations of the above data with the grid SICs. The daily (5 days) grid SIC data also indicated that the annual maximum sea ice area in the whole and southern Okhotsk Sea mostly covaried with each other, including the abrupt reduction in 1989/1990 (Tachibana *et al.*, 1996) and the recent peak in 2001. In addition, these interannual variations were reflected in the yearly accumulated SIC (Aota *et al.*, 1988) and sea ice duration variations along the Okhotsk coast of Hokkaido. The long-term sea ice duration time series suggested that the decadal-scale relationships of the above sea ice indices to the indices for the North Pacific climate mode variabilities varied with time. Among several climate indices, the NPI is a robust indicator of recent (after the 1980s) sea ice variations in the Sea of Okhotsk. We also examined the differences between the start and end date variations, which determine the durations. Variations in the start date at the Okhotsk coast sites resulted from the variations in the Aleutian Low strength, the air temperature around Japan in January, and partly the SST along the Soya warm current in December. Variations in the end date resulted from the Aleutian Low variations; the sea ice cover variations affected the air temperatures over the Sea of Okhotsk in April, in contrast to the sea ice cover variations in January resulting from the air temperature variations.

Although further investigation is necessary (such as for quantitative evaluation of the causal factors, and dependencies among them), our results highlighted the interactive linkage between variations in the sea ice along the Okhotsk coast of Hokkaido and large-scale fields, which will help improve our understanding of the sea ice extent and retreat variability in the Sea of Okhotsk. This study implies that the long-term observation data at the JMA meteorological observatories are highly valuable for climate study, especially on the decadal and longer time scale climate variability in the North Pacific. We hope this study provides interdisciplinary feedback to the operational monitoring of the sea ice. In addition, reproduction of the sea ice along the Okhotsk coast of Hokkaido is one of the issues to be improved in the operational forecasting system of the JMA (Hirose *et al.*, 2019). The results of this study might help specify the processes that are necessary for improvement in this region and the data can be a beneficial source for initializing the forecast system. This study is a first step toward accomplishing these objectives.

Acknowledgements

We are grateful to two anonymous reviewers and editors, Hiromitsu Kitagawa (Ocean Policy Research Institute) and Shuhei Takahashi (Okhotsk Sea Ice Museum of Hokkaido) for their constructive comments. We acknowledge Fumitake Shido (Sapporo District Meteorological Observatory, JMA) for providing helpful information on the operational sea ice monitoring at the Abashiri Local Meteorological Observatory. We also thank Tomonori Tanikawa (Department of Physical Meteorology Research, Meteorological Research Institute, JMA) and Takenobu Toyota (Institute of Low Temperature Science, Hokkaido University) for their fruitful discussion on the sea ice variability in the southern Okhotsk Sea. We are indebted to Shuhei Takahashi, Eriko Uematsu, and Mombetsu City for long being involved in organizing the International Symposiums on the Okhotsk Sea and Polar Oceans. This study was supported by the Japan Society for the Promotion of Science (KAKENHI Grant Number 20K12142 and 20H01968), and by the ArCS II Project (Program Grant Number JPMXD1420318865) of the Japanese Ministry of Education, Culture, Sports, Science and Technology.

References

Aota, M., M. Ishikawa and E. Uematsu (1988): Variation in ice concentration off Hokkaido Island. *Low Temp. Sci., Ser. A*, **47**, 161-175.

Aota, M. and M. Ishikawa (1993): Data on the variation in ice concentration along the Okhotsk Sea coast of Hokkaido. *Sea and Sky*, **69**, 33-46 (in Japanese).

Aota, M. (1999): Long-term tendencies of sea ice concentration and air temperature in the Okhotsk Sea coast of Hokkaido. *PICES Scientific Report*, **12**, 1-2.

Di Lorenzo, E. and 11 co-authors (2008): North Pacific Gyre Oscillation links ocean climate and ecosystem change. *Geophys. Res. Lett.*, **35**, L08607.

Hirose, N. and 9 co-authors (2019): Development of a new operational system for monitoring and forecasting coastal and open-ocean states around Japan. *Ocean Dyn.*, **69**, 1333-1357.

Honda, M., K. Yamazaki, Y. Tachibana and K. Takeuchi (1996): Influence of Okhotsk sea-ice extent on atmospheric circulation. *Geophys. Res. Lett.*, **23**, 3595-3598.

Honda, M., K. Yamazaki, H. Nakamura and K. Takeuchi (1999): Dynamic and thermodynamic characteristics of atmospheric response to anomalous sea-ice extent in the Sea of Okhotsk. *J. Clim.*, 12, 3347-3358.

Honda, M. (2007): Relationship between the Okhotsk sea ice and atmospheric field. *Kishou Kenkyu Note*, **214**, 63-73 (in Japanese).

Kawasaki, K., Y. Tachibana, T. Nakamura and K. Yamazaki (2021): Role of the cold Okhotsk Sea on the climate of the North Pacific subtropical high and Baiu precipitation. *J. Clim.*, **34**, 495-507.

Kimura, N. and M. Wakatsuchi (1999): Processes controlling the advance and retreat of sea ice in the Sea of Okhotsk. *J. Geophys. Res.*, **104**, 11137-11150.

Kurihara, Y. and 2 co-authors (2006): Global daily sea surface temperature analysis using data from satellite microwave radiometer, satellite infrared radiometer and in situ

observations. *Wea. Bull.*, **73**, 1-18 (in Japanese).
Kobayashi, S. and 11 co-authors (2015): The JRA-55 Reanalysis: general specifications and basic characteristics. *J. Meteorol. Soc. Jpn.*, **93**, 5-48.
Mantua, N. J. and S. R. Hare (2002): The Pacific Decadal Oscillation. *J. Clim.*, **18**, 4355-4373.
Nakamura, K. (1996): Quantitative understanding of the cooling effect of sea ice on the temperature in the coastal area of the Sea of Okhotsk in Hokkaido. *Tenki*, **43**, 383-390 (in Japanese).
Nakamura, T., T. Toyoda, Y. Ishikawa and T. Awaji (2006): Enhanced ventilation in the Okhotsk Sea through tidal mixing at the Kuril Straits. *Deep-Sea Res. I*, **53**, 425-448.
Ohshima, K. I., T. Watanabe and S. Nihashi (2003): Surface heat budget of the Sea of Okhotsk during 1987-2001 and the role of sea ice on it. *J. Meteorol. Soc. Jpn.*, **81**, 653-677.
Ohshima, K. I., S. Nihashi, E. Hashiya and T. Watanabe (2006): Interannual variability of sea ice area in Sea of Okhotsk: Importance of surface heat flux in fall. *J. Meteorol. Soc. Jpn.*, **84**, 907-919.
Ohshima, K. I., T. Nakanowatari, S. Riser, Y. Volkov and M. Wakatsuchi (2014): Freshening and dense shelf water reduction in the Okhotsk Sea linked with sea ice decline. *Prog. Oceanogr.*, **126**, 71-79.
Ohshima, K. I., D. Shimizu, N. Ebuchi, S. Morishima and H. Kashiwase (2017): Volume, heat, and salt transports through the Soya Strait and their seasonal and interannual variations. *J. Phys. Oceanogr.*, **47**, 999-1019.
Parkinson, C. L. and D. J. Cavarieri (2008): Arctic sea ice variability and trends, 1979-2006. *J. Geophys. Res.*, **113**, C07003.
Shevchenko, G. V., A. B. Rabinovich and R. E. Thomson (2004): Sea-ice drift on the northeastern shelf of Sakhalin Island. *J. Phys. Oceanogr.*, **34**, 2470-2491.
Shirasawa, K., M. Lepparanta, T. Saloranta, T. Kawamura, A. Polomoshnov and G. Surkov (2005): The thickness of coastal fast ice in the Sea of Okhotsk. *Cold Reg. Sci. Technol.*, **42**, 25-40.
Tachibana, T., M. Honda and K. Takeuchi (1996): The abrupt decrease of the sea ice over the southern part of the Sea of Okhotsk in 1989 and its relation to the recent weakening of the Aleutian low. *J. Meteor. Soc. Jpn.*, **74**, 579-584.
Takahashi, S., T. Kosugi and H. Enomoto (2011): Sea-ice extent variation along the coast of Hokkaido, Japan: Earth's lowest-latitude occurrence of sea ice and its relation to changing climate. *Ann. Glaciol.*, **52**, 165-168.
Toyoda, T. and 34 co-authors (2017): Interannual-decadal variability of wintertime mixed layer depths in the North Pacific detected by an ensemble of ocean syntheses. *Clim. Dyn.*, **49**, 891-907.
Toyota, T., N. Kimura, J. Nishioka, M. Ito, D. Nomura and H. Mitsudera (2021): The interannual variability of the ice conditions in the southern Sea of Okhotsk and its likely factors. Jpn. Oceanogr. Soc. 2021 Fall Meeting, 21F-05-1 (14 Sept. 2021).
Trenberth, K. E. and J. W. Hurrell (1994): Decadal atmosphere-ocean variations in the Pacific. *Clim. Dyn.*, **9**, 303-319.
Wallace, J. M. and D. S. Gutzler (1981): Teleconnections in the geopotential height field during the northern hemisphere winter. *Mon. Wea. Rev.*, **109**, 784-812.
Watanabe, T. (1990): Study on formation processes of SST anomalies in the western North Pacific: Role of the East Asian winter monsoon. Doctoral Thesis, Tohoku University, 121 pp. (in Japanese).
Yamazaki, K. (2000): Interaction between the wintertime atmospheric circulation and the variation in the sea ice extent of the Sea of Okhotsk. *Seppyo*, **62**, 345-354 (in Japanese).

Correspondence to: T. Toyoda, ttoyoda@mri-jma.go.jp